DIGITAL CORE SIMULATOR – A PROMISING METHOD FOR DEVELOPMING HARD-TO-RECOVER OIL RESERVES TECHNOLOGY

V.B. Betelin[1], V.A. Galkin[1], A.V. Shpilman[2], N.N. Smirnov[1,3*]

[1]Federal Science Center Scientific Research Institute for System Analysis of Russian Academy of Sciences, 36-1, Nakhimovskiy pr., Moscow, 117218, Russia

[2]V.I.Shpilman Research and Analytical Center for the Rational Use of the Subsoil, 75, Malygina, Tyumen, 625026, Russia

[3]Lomonosov Moscow State University, GSP-1, Leninskie Gory, Moscow, 119991, Russia

*e-mail: ebifsun1@mech.math.msu.su

Abstract. Territory of Russia, which occupies 12.8% of the Earth's territory, contains 12-13% of the forecast resources, and about 12% of the discovered oil reserves. Russia's proven oil reserves amount to approximately 13.9 billion tons of oil as of January 1, 2017 (~101 billion barrels). Oil recovery factor for proved reserves is ~17%. The increase of oil recovery factor represents a huge stockpile for raising the level of oil production in the country at low costs. Creation of improved core-simulator designed for indigenous supercomputers, with the opportunity to take advantage of various methods of speeding up the numerical simulations process is one of the most burning issues in the development of strategic reserves of hydrocarbons in our country. The paper gives a coverage of results of computer simulations of different strategies relevant to enhancing oil recovery from host rock formations.
Keywords: oil deposit, oil reserves, oil recovery factor, numerical simulations, core-simulator, micro-scale

1. Introduction

At the moment Russia maintains a leading place in oil production. In 2011, oil production in Russia amounted to 510 million tons, and in 2017 – increased to 546.7 million tons. Along with Russia's economic growth, the demand for oil will increase. According to the forecasts of the Energy Strategy of Russia until 2030, the oil industry of the country will produce at least 500 million tons of oil under different scenarios. This will require an increase in reserves at a level not lower than oil production. If the market situation worsens or politically motivated state decisions are taken at the international level, oil production in Russia may fall below 500 million tons, but such scenarios seem unlikely.

The share of so-called hard-to-recover reserves (HTR reserves) in the total balance of Russia's residual oil reserves is large. HTR reserves include, among other things, the reserves with lower reservoir filtration and capacity properties and, accordingly, the rates of recovery, which are several times lower than those achieved in fields with more favorable conditions for development. HTR reserves accounts for about 50% of Russia's known reserves. Oil production from them is currently ~8% per year.

Residual reserves of developed deposits are characterized in Russia by a number of negative features:

• high degree of depletion, which exceeds 50% at many fields,

• high water cut - about 70% on average.

The ratio of oil production to prove reserves of the domestic oil industry is ~ 27 years. This is a good reserves-to-production ratio, but production at the level of ~ 500 million tons per year will require additional efforts for reserves growth, given the fact that the quality of the remaining reserves is deteriorating.

The question arises inevitably: are we using explored and developed oilfields effectively? Do we provide sufficient recovery of hydrocarbons, particularly as regards oil?

The main objective reason for the low oil recovery rate relates to the fact that different parts of the rocks have different resistance to the flow of reservoir fluids – oil, gas and water, that is, they have "filtration heterogeneity". This leads to the emergence of stagnant zones, or, in professional terms, "bypassed oil". After such stagnant zones were "bypassed" by stratal water or water specially injected into the reservoir to displace oil, they are almost never not involved in oil production.

Such stagnant zones have different spatial dimensions: from pore scales (i.e. from fractions of a micron to fractions of a millimeter) – "micro-cells"; to the scales of geological interlayers and layers (i.e. from a centimeter to several meters); and to the scales of the distance between oil wells (i.e. from tens to hundreds of meters).

Reduction of oil recovery factor (ORF) is also possible due to the viscous instability of the displacement front, since the displacing agent (water) has a lower viscosity than oil. This leads to the appearance of the "tongues" of the displacing fluid, embracing the stagnant zones of oil.

The increase in oil recovery is a huge reserve to increase the level of oil production in the country at a lower cost. Most of the residual reserves remain in the fields after development finishing in meso- and macro-scale stagnant zones and lenses, which are, in principle, the reserves of additional production. If even one assume that it will be possible to increase ORF by 5% – from 17% to 23%, then it will become possible to produce additionally ~4 billion tons of oil.

There are five groups of enhanced oil recovery methods have been developed and being used to date on an industrial scale:

- in-fill drilling (including directed sidetrack drilling);

- gas methods (injection of hydrocarbon gases, carbon dioxide, nitrogen, flue or other gases injected into the reservoir both neat and in a mixture with liquids);

- physical and chemical methods (different types of flooding: with surfactants, polymers, micellar; injection of liquid solvents; injection of other chemicals: acids, alkalis, salt solutions, etc.);

- thermal methods (displacement of oil by heat carriers, impact with exothermic oxidizing or other intrastratal reactions).

- microbiological methods (injection of bacterial products into the reservoir or its formation directly in the reservoir).

The so-called unconventional reservoirs, such as siliceous-argillaceous and calcareous-siliceous-argillaceous oil-saturated rocks of the Bazhenov formation, are also strategically highly prospective. Today, several methods for the development of such deposits are considered:

- oil production with traditional methods from high-permeable differences and pores of the rock matrix, currently applied in Western Siberia;

- application of hydraulic fracturing (of different design) to increase the oil flow rates and increase the drained rock volumes;

- creation of a combustion source in the reservoir with air injection (thermal gas treatment). The processes occurring in the reservoir during thermal gas treatment are yet to be fully studied. Some researchers suppose that there is a transformation of kerogen into oil and gas.

Extraction of the remaining oil requires a comprehensive approach. It is necessary to optimize the stimulations (mechanical, thermal, chemical), which effect on the reservoir to increase an oil recovery factor. Of course, these parameters can be chosen empirically, but a limited number of experiments and the high cost of in-situ tests make the task difficult.

At the moment, none of the existing simulators can effectively carry out calculations using a fine-mesh adaptive grid with cell sizes in centimeters and even less, millimeters, i.e. it is impossible to study the formation at the micro level. Also, commercial simulators do not allow effective calculation of filtration processes taking into account non-equilibrium phase transformations and non-equilibrium chemical reactions. Modern simulators are not adapted for parallelization on supercomputers. Most of them are focused on the use of ordinary personal computers with one processor. In this case, the calculation of only one option: a) when modeling in-situ combustion on a relatively small grid, or b) calculation of a simple isothermal two-phase filtration for a large field (about 1000 wells) with a 25m cells grid on the PC takes months, and on cluster systems – weeks. When designing or managing development, the design options are number in tens.

In addition, using of the foreign termohydrosimulators bears the risk of inability of their use, or improvement, or adaptation to other different conditions or tasks in the event of a change in the geopolitical situation and appearing of additional difficulties in contacts between governments of developer countries. This situation is unacceptable for the development of our country's strategic hydrocarbon reserves.

For the successful creation of a multiscale thermohydrosimulator, it is necessary to know how to describe in detail the flow and interaction of the fluids and porous rock matrix in the small scales comparable to the scales of the cores extracted during drilling. This task gave an impetus to the development by the leading world laboratories of the so-called core simulators.

Thus, the creation of an improved, own in house core simulator developed for domestic supercomputers, with the opportunity to use various methods of accelerating the calculations is one of the most important elements in the development of strategic reserves of hydrocarbons in our country.

A consortium was created to solve the problem of the core simulator including the Federal scientific center "Scientific-Research Institute for system analysis RAS" (Moscow), Moscow M.V. Lomonosov state University. (Moscow), V.I. Shpilman Research and Analytical Center for the Rational Use of the Subsoil (Khanty-Mansiysk, Tyumen), LLC "Center for computational modeling" – a resident of SKOLKOVO (Zelenograd) and Surgut state University (Surgut). Having combined fundamental and practical knowledge in the field of mathematics, mechanics, computer systems, geology and geophysics, the consortium set itself the task to create a program complex "core simulator" in the framework of the project "Digital deposit", including the validation of numerical results on its own experimental basis and development of technology for modeling changes in the reservoir at the micro level when exposed to stimulations in different ways - heating, injection of reagents, hydraulic fracturing, etc.

The consortium published a number of articles on the subject of studies [1,5-11] and organized the following scientific events, at which the results of joint activities were presented:

- All-Russian scientific conference "Digital Core Model" (Moscow, 2017);

- section within the framework of the International Conference "Mathematics and Information Technologies in the Oil and Gas Complex" (Surgut, 2016),

- XX scientific and practical conference "Ways of realizing the oil and gas potential of the Khanty-Mansiysk Autonomous region- Ugra" (Khanty-Mansiysk, 2016);

- Working group meetings in Khanty-Mansiysk (2015), Surgut (2015), Tyumen (2015), Tobolsk (2015), Suzdal (2016).
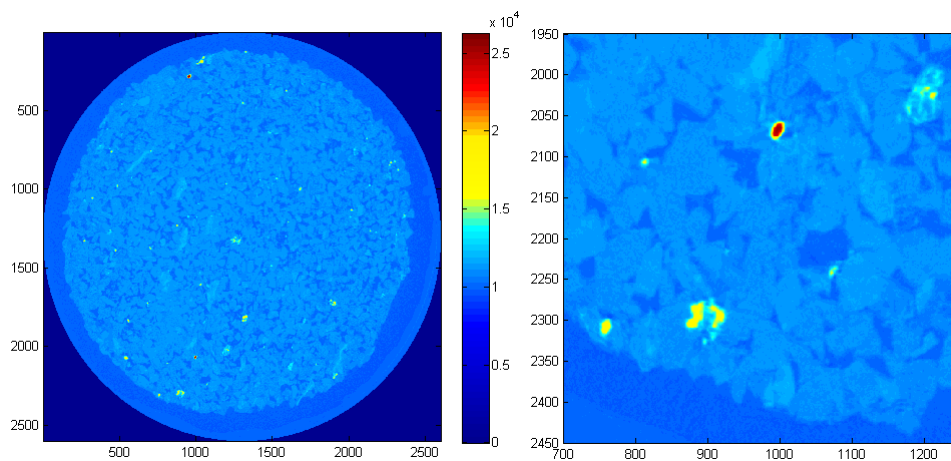

Fig. 1. Core samples (sandstone)

Fig. 2. Results of X-ray tomography

As a result of the cooperation of organizations within the consortium, the following results were obtained.

2. Reconstructing structure of the pore space based on tomography data

Based on the results of tomography of core samples (sandstone) (Fig. 1, Fig. 2) a method of reconstructing of the structure of the pore space in a core sample from the data of its x-ray tomography was developed. As the initial data, the absorption coefficient of x-ray radiation by the core sample given in the 16-bit format was considered. Physically, the sample was a

core with a diameter of about 8 mm and a length of about 19 mm. In numerical form, after x-ray tomography and restoration of the x-ray absorption coefficient, the sample was divided by a square grid of 2600×2600×6360 cells (about 43 billion cells). From these data, the structure of channels and pores was further distinguished on the basis of the selection of the threshold value of the x-ray absorption coefficient, i.e. it was believed that everything above the threshold value in the considered area is a rock matrix; and everything below is a pore space. An example of such a structure is presented on Fig. 3.

a   b
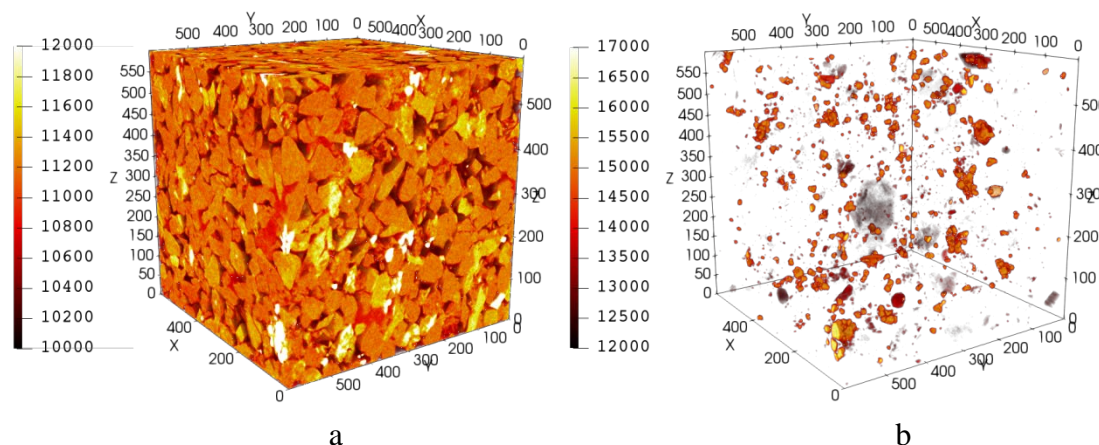
Fig. 3. Results of reconstructing of the structure of the pore space in a core sample with size 1.79376 mm (600^3 cells) for threshold value: a) 10000-12000; b) 12000-17000

For visualizing tomography data, we developed a special package PoreProject (Fig. 4). The package allows you to visualize the internal structure of the core sample, as well as examine different parts and sections of the object. In comparison with similar packages, PoreProject is designed specifically for core structure visualization and can process much larger data sets.
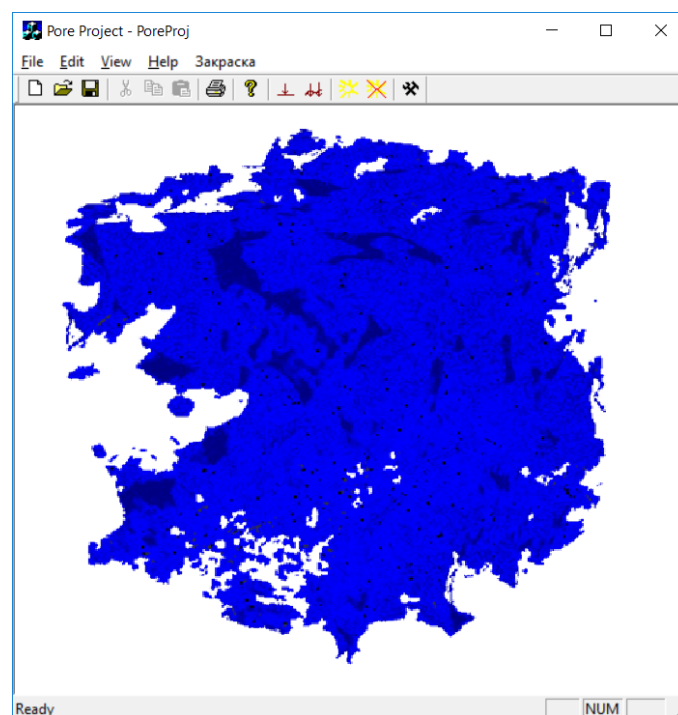

Fig. 4. PoreProject visualization package developed by Federal Science center - Scientific research Institute for system Analysis, Russian Academy of Sciences

In the obtained structure of the pore space, the numerical simulation of the fluid flow based on the Stokes model for an incompressible fluid was carried out (Figs. 5-6). The possibility of such modeling is extremely relevant since various studies of real rock samples are very time-consuming and complex tasks, and associated with a number of difficulties. For example, some of these studies are the "single-actions" and lead to the impossibility of re-experiment, or any other experiments and to the complete destruction of the test sample. In this regard, the possibility of modeling flows within the "digital core" is of considerable interest, as allows to execute any number of complex experiments and is currently limited only by computational resources.

a   b
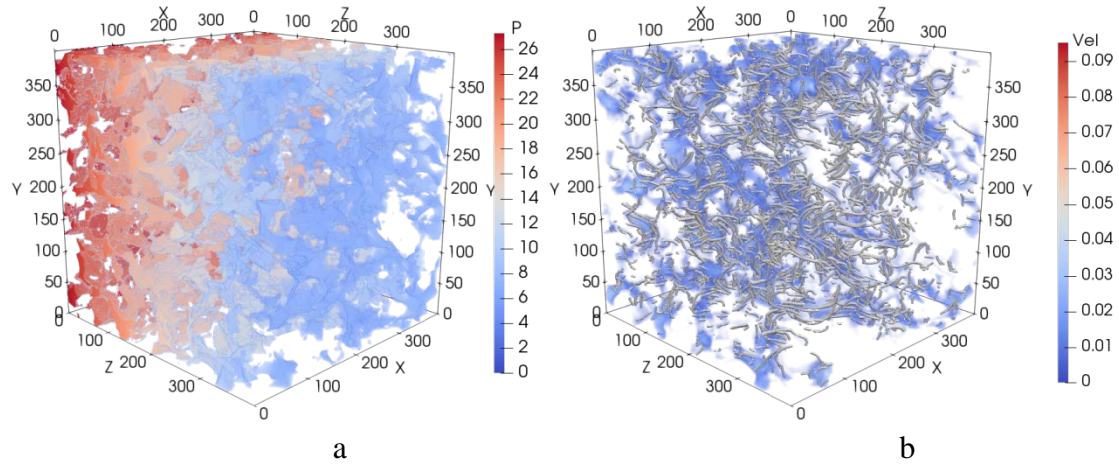
Fig. 5. Distribution of dimensionless parameters: a) pressure and b) velocity with streamlines for core samples with 1.19584 mm size (400^3 voxels) for threshold value 10500

The mathematical model of the problem was the Stokes hydrodynamic model for incompressible fluid and steady-state flows. The following system of dimensionless equations was considered:

$$\operatorname{div} \mathbf{u} = 0, \quad \Delta \mathbf{u} = \nabla p, \tag{1}$$

where $\mathbf{u}$ – velocity vector, p – pressure.

At the open boundaries of the channels extending to the edge of the computational domain under consideration, the conditions of the free boundary for the velocity and the pressure distribution with a single modulus of the gradient vector and depending on its direction were specified. The pressure at the point O (0,0,0) located in one of the corners of the cube under consideration was taken as the zero level of pressure. In the remaining boundary regions of the computational domain, the condition of zero velocity was set for all components (sticking to the walls).

To determine the dimensionless permeability, the following relationships were used:

$$\Xi = \mathbf{T} \cdot \mathbf{v}, \quad \mathbf{v} = \left(\frac{q_x}{S_{yz}}, \frac{q_y}{S_{xz}}, \frac{q_z}{S_{xy}} \right), \quad \mathbf{T} = \nabla p = \left(t_x, t_y, t_z \right), \tag{2}$$

here $\mathbf{v}$ – seepage velocity vector, $\mathbf{T}$ – pressure gradient direction, $\mathbf{q} = \left(q_x, q_y, q_z \right)$ – total incoming flow on the faces normal to the corresponding coordinate vector. The porosity of the structure obtained was defined as the ratio of the volume occupied by the selected channels and pores involved in the simulation to the volume of the entire piece cut from the original sample.
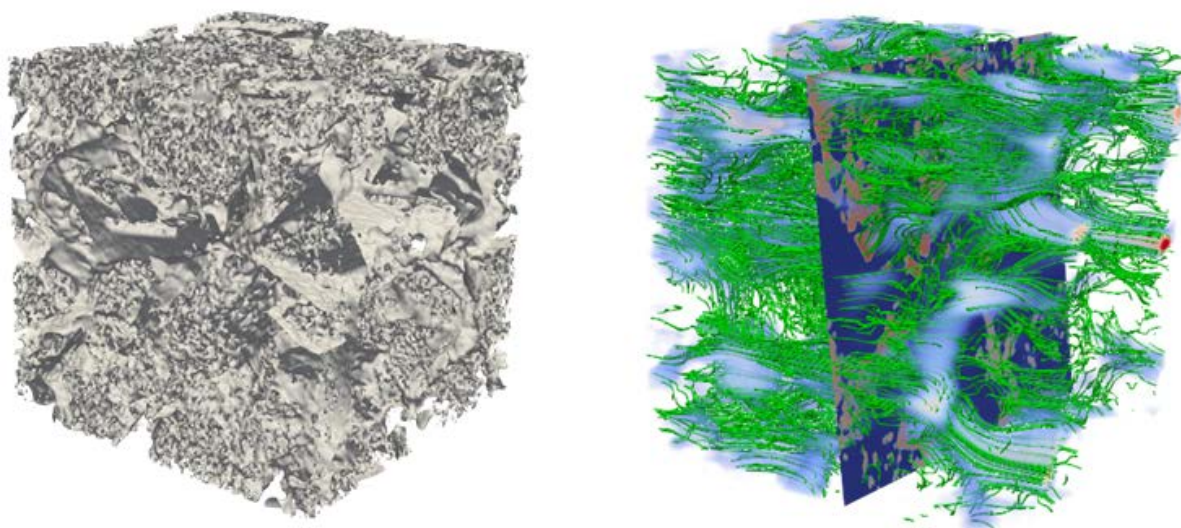
Fig. 6. Modeling of the flow in the pore space of a core sample

At the moment, work is underway to assess the porosity and permeability of the pore and channel system obtained as a result of x-ray tomography processing, and to select the optimal threshold value of the x-ray absorption coefficient, on the basis of which the pore space and the solid skeleton are separated.

When considering the reconstructed structure for a region randomly cut from the entire sample, it was obtained that with an increase in the size of the cut region, the calculated permeability value is in a rather wide range (Fig. 7). In total, several series of numerical experiments were carried out for cubes with sides of 0.29896, 0.59792, 0.89688, 1.19584, and 1.4948 mm in hundreds of random cuts for each size.
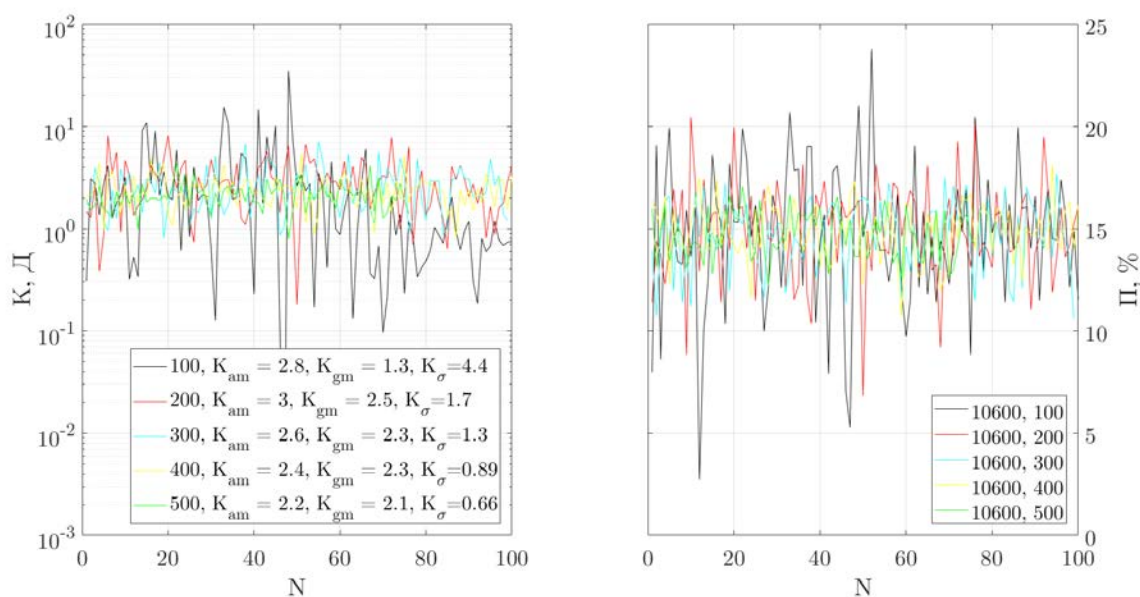
Fig. 7. Permeability of the restored pore space structure for several random samples for threshold value 10600

It was found that the value of permeability itself fluctuates over a fairly wide range of values, and the standard deviation for each series of numerical experiments decreases with increasing size of the cube under consideration. Thus, it can be concluded that when considering a region of too small a size, the permeability estimate may not be objective due to comparable pore sizes and the region itself. For an adequate assessment of the permeability of the entire specimen based on considering the small region cut out, it is necessary to consider the region of a sufficient volume.

Natural experiments on displacement of oil modeling fluids with water from Neocomian sandstones were also carried out. The oil modeling fluid (oil or kerosene) was displaced from the core under the influence of a constant pressure gradient or with a constant flow rate. The process of oil displacement was numerically simulated, the results of calculations were compared with experimental data [10]. On the basis of the experimental results the coefficients for the accounting of capillary effects in the mathematical model used in numerical modeling were selected.

3. Students workshop on modeling of oil displacement

On the basis of the conducted research, an interactive workshop was created for students studying oil and gas specialties (Fig. 8). The workshop allows students to model the flow of viscous liquids in core samples at the macro level in the program with a convenient interface. In the process of performing the tasks of the workshop, students study the influence of various parameters on the process of displacement of oil from the pore space, explore the possibilities of increasing the displacement coefficient. Students can compare the results of the simulation with the built-in results of experiments on the displacement of oil models with water from the Neocomian sandstones.
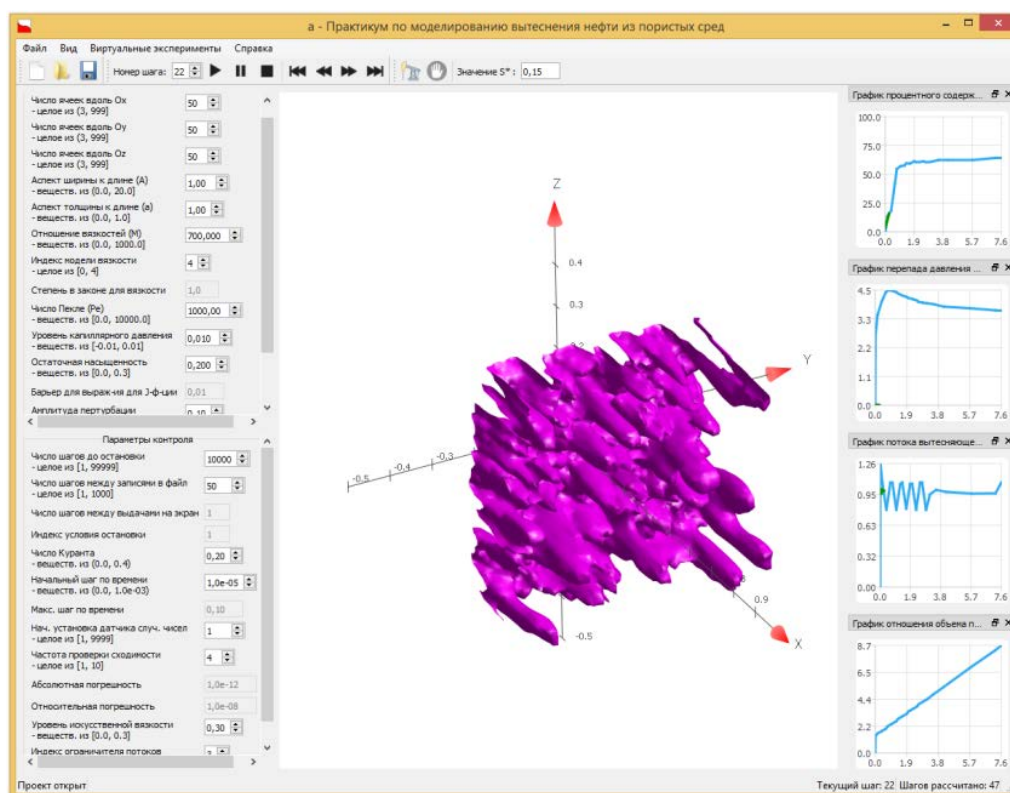

Fig. 8. Students workshop on modeling of oil displacement from porous media developed by Federal Science center – Scientific research Institute for system Analysis, Russian Academy of Sciences

4. The digital simulator for displacement of viscous fluids from porous media

One of the technologies for the extraction of liquid minerals involves displacing them from porous formations under the action of a pressure gradient. However, when displacing a more viscous fluid (oil) with a less viscous (water) fluid, the displacing fluid tends to break through the layer of displaced, forming channels in it called "viscous fingers". The resulting instability leads to the destruction of the initially flat shape of the interface and the breakthrough of individual fingers of the displacing fluid, which significantly affects the quality of oil production. In this part of the article, we will consider a numerical and experimental study of the displacement of viscous liquids from a porous medium, taking into account capillary effects and instability of the displacement front.

The flow of two incompressible fluids in the pore space is considered. Thermal effects are not taken into account. The seepage flow is modeled by Darcy's law, taking into account the capillary effects at the phase interface. The permeability and porosity depend on spatial coordinates. The mathematical formulation of the problem describes the displacement of fluid by another fluid due to the pressure drop, either due to capillary effects.

Equations of mass balance of phase k are as follows:

$$\frac{\partial \varphi s_k \rho_k}{\partial t} + \frac{\partial}{\partial x_j}\left(\rho_k u_{k,j}\right) = 0.$$

Here ρ_k – is the true phase density, s_k – is the phase saturation, $u_{k,j}$ – is the component j of the phase filtration velocity. In the equations, the summation over the repeating index j is carried out.

The average volume filtration velocity u_j is defined as:

$$u_j = \sum_k u_{k,j}.$$

Darcy's Law:

$$u_{k,j} = -\frac{K k_k}{\mu_k}\frac{\partial p_k}{\partial x_j},$$

where p_k – phase pressure.

The capillary pressure is modeled by the Leverette model:

$$p^C = p_O - p_w = C_J \frac{\sigma|\cos\theta|}{\sqrt{K/\varphi}} \cdot \begin{cases} S^{-a_J}, & \cos\theta > 0; \\ (1-S)^{-a_J}, & \cos\theta < 0. \end{cases}$$

We introduce the reduced pressure p and the auxiliary function $\xi(s)$ so that the pressure in each phase is expressed as follows:

$$p_w = p + \xi(s) - p^C/2,$$
$$p_O = p + \xi(s) + p^C/2.$$

Then for the average volume filtration velocity we get:

$$u_j = -K\big(M_O(s) + M_w(s)\big)\frac{\partial p}{\partial x_j}.$$

The auxiliary function $\xi(s)$ is found from the expression:

$$\frac{d\xi(s)}{ds} = \frac{1}{2}\frac{M_w(s) - M_O(s)}{M_w(s) + M_O(s)}\frac{dp^C(s)}{ds}.$$

The mobility is found by the Brooks-Corey model:

$$M_O(s) = \frac{k_O}{\mu_O}S^{n_O},$$
$$M_w(s) = \frac{k_w}{\mu_w}(1-S)^{n_w},$$

where S – effective saturation.

For the coefficient of capillary force d_C we have:

$$d_C = -K\frac{M_O M_w}{M_O + M_w}\frac{dp^C(s)}{ds} = \frac{C_J a_J|\cos\theta|\sigma\sqrt{K\varphi}M_O M_w}{(s_{max} - s_{min})(M_O + M_w)} \cdot \begin{cases} S^{-1-a_J}, & \cos\theta > 0; \\ (1-S)^{-1-a_J}, & \cos\theta < 0. \end{cases}$$

Displacing phase flow:

$$u_O = -KM_O \frac{\partial p}{\partial x_j} - d_C \frac{\partial s}{\partial x_j}.$$

The empirical constants in the mathematical model can be determined experimentally. Experiments on the displacement of a viscous liquid from a core (a sample of a porous medium) were carried out at the V.I. Shpilman Research and Analytical Center for the Rational Use of the Subsoil. Experiments described in detail in [10]. To conduct a series of experiments on the PLAST.ATM-10 installation (Fig. 9), a composite sample of Neocomian sandstone with a length of 0.1 m was used. Two fluids were chosen as models for oil: kerosene (experiments No. 1 and No. 3) and hydraulic oil (experiments No. 2 and No. four). Distilling water was chosen as the displacing fluid. The core sample was composed of three cylindrical samples. In each experiment, a sample of a porous medium was initially saturated with an oil model and then, at a constant flow rate (experiments No. 1 and No. 2) or at a constant pressure drop (experiments No. 3 and No. 4), displacement occurred.
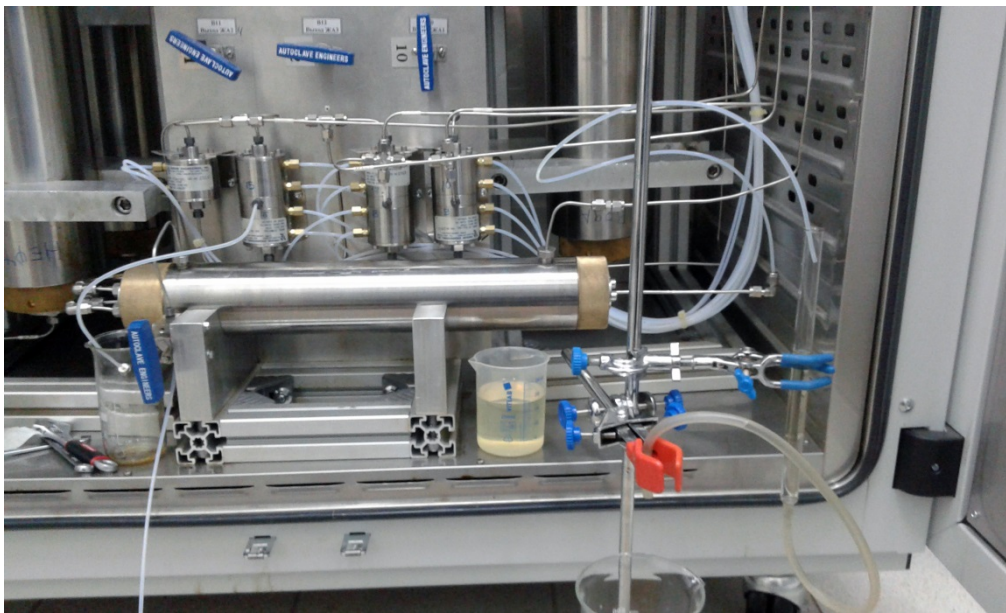

Fig. 9. Installation for carrying out experiments to displace a viscous fluid from a sample of a porous medium

Figure 10 presents the comparison of results of numerical simulations based on the described mathematical model with experimental data.

In the case the constant flow rate is chosen as the boundary condition, (Fig. 10a and Fig. 10b) the difference between the result of numerical calculations and the experiment is not significant. The difference for the case of constant pressure at the boundary (Fig. 10c and Fig. 10d) can be explained by the heterogeneity of the core material used for the experiment (in the numerical model, the area was assumed to be uniform, with constant permeability). As a result of the non-uniformity of the core, an area in which displacement occurs faster could be formed in the core, while in numerical calculation, displacement occurs uniformly in the entire region. It can also be caused by the fact that the core sample is a compound and, in the case of a constant pressure drop, the presence of joints could have an effect on the displacement process.
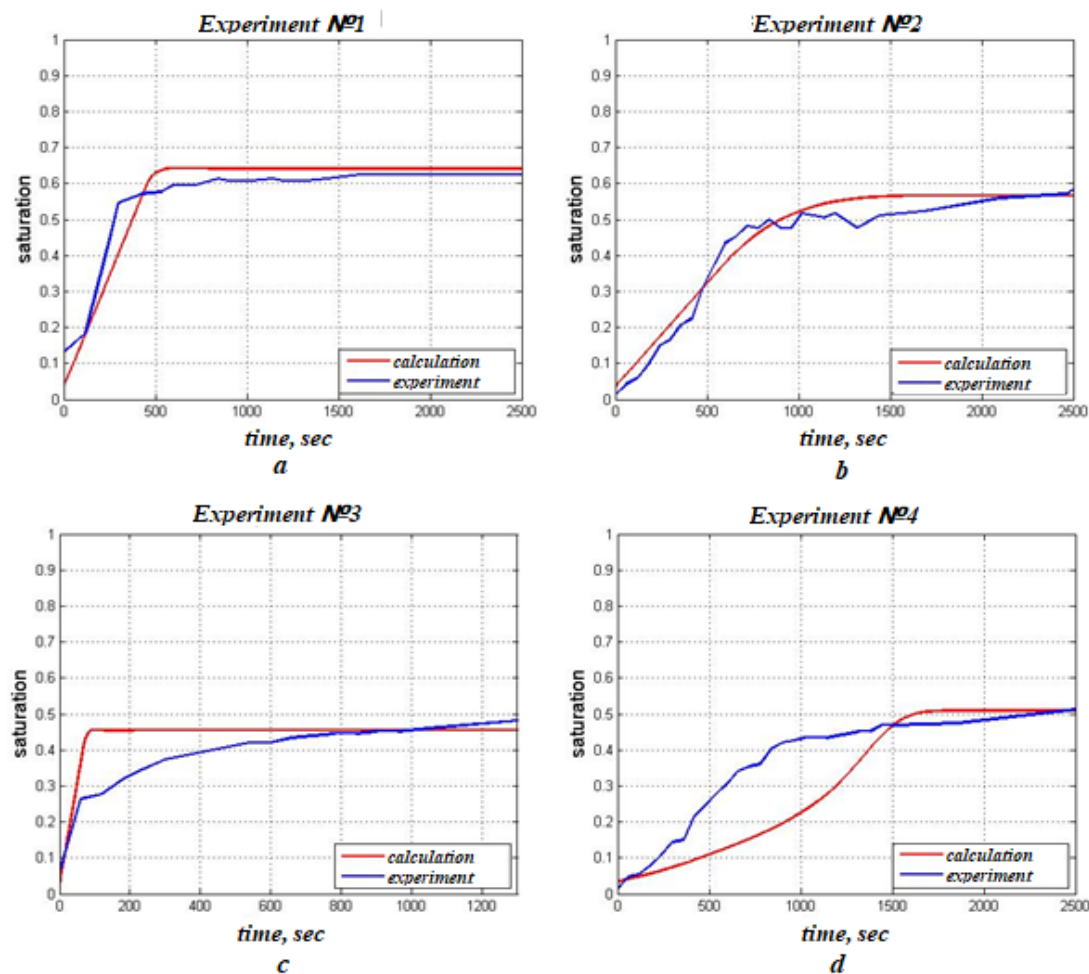
Fig. 10. Comparison of the results of the experiment on the displacement of fluid from the core with a numerical calculation

Figures 11(a)-11(c) show how the shape of the interface of the displacing and displaced liquids changes with time in calculations corresponding to the experiments.

Figure 11a shows the change in the shape of the interface in the numerical calculation for the case of the displacement of kerosene with water at a constant flow rate (experiment No. 1). For the case of displacing kerosene with water at a constant pressure drop (experiment No. 3), the picture is similar: the ratio of viscosity of liquids is close to 1, so the interface remains flat at any moment in time (the ideal case of displacement is possible in theory, but never realized in practice). Figures 11 (b) and 11 (c) correspond to experiment No. 2 and No. 4, respectively. In these cases, due to the large viscosity ratio ($\approx$25), instability is observed, which develops at the displacement front.

Thus, as a result of the comparison of data from supercomputer modeling of oil displacement from rock samples with a laboratory experiment to displace oil replacing liquids with water, it is possible in principle to determine unknown parameters of the model, such as the capillary characteristics of the rock and saturating liquids.
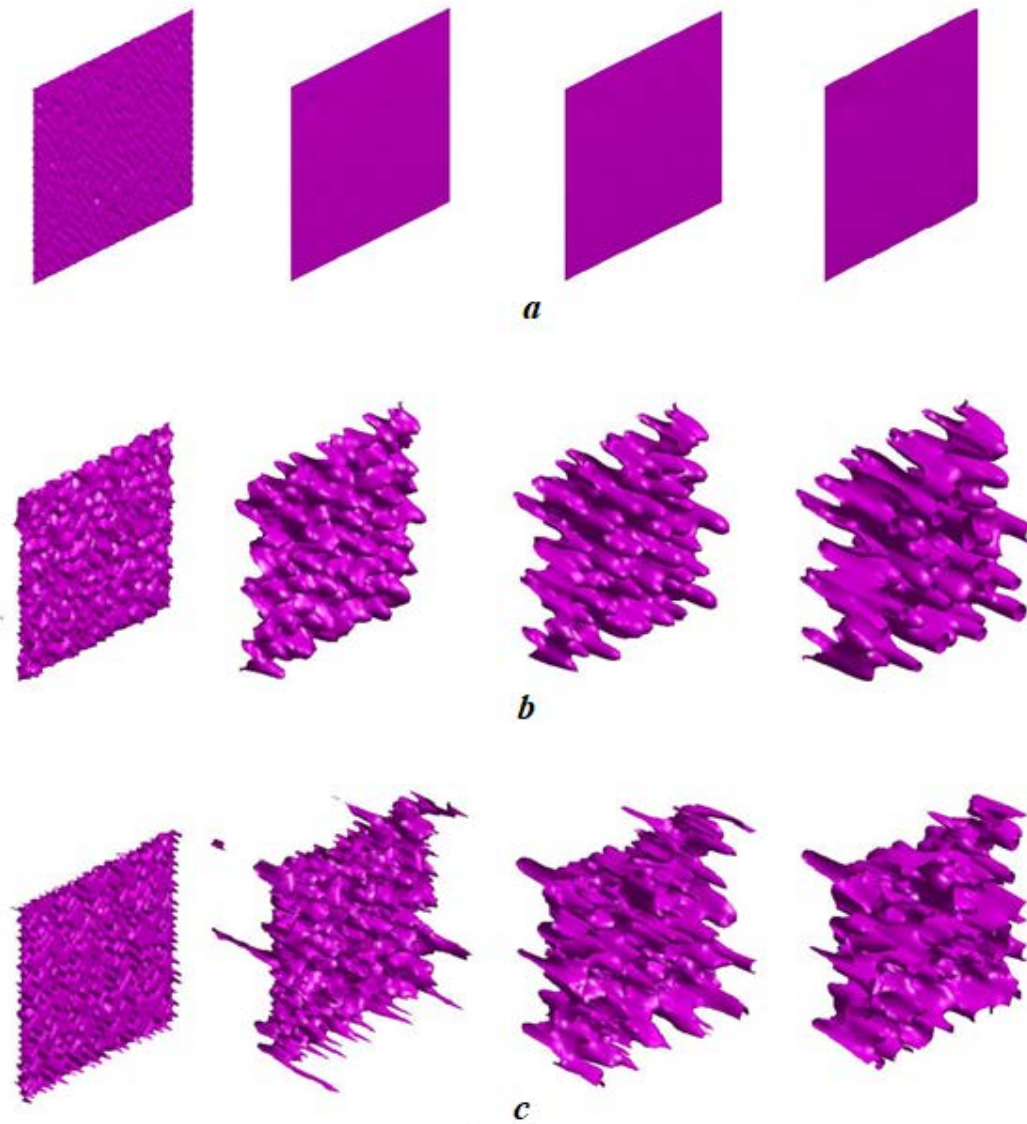
Fig. 11. The shape of the interface of liquids for numerical calculations

5. The estimates of the effect of hydraulic fracturing on the dynamics of oil displacement
The displacement modeling methods described above provide an opportunity to investigate the effect of fracture on the quality and rate of oil production. Two series of calculations were carried out, differing by the relative position of injection and production wells. In each series of calculations, a different number and position of fractures was considered. The purpose of comparing the results was to show how the presence or absence of such a method of intensifying oil production, like hydraulic fracturing, affects the dynamics of oil recovery, including the final well production.

In the first series of calculations, a rectangular area with a size of 300m × 500m containing two wells (producing and injecting) located at a distance of 200m from each other was considered. There may be one or two fractures near the production well. The length of each crack was 100 meters. The permeability and porosity of the medium are respectively $5 \cdot 10^{-13} \ m^2$ and 0.2. The permeability and porosity of the crack, respectively, $5 \cdot 10^{-11} \ m^2$ and 0.4. The pressure on the injection wells is $5 \cdot 10^7$ Pa, on the production well $5 \cdot 10^5$ Pa. Five calculations were carried out: 1 for the absence of a crack, 3 for a different position of

the crack and 1 for the case of two cracks. Figure 12 shows the water saturation at different points in time for each calculation (α is the angle of inclination of the fracture).
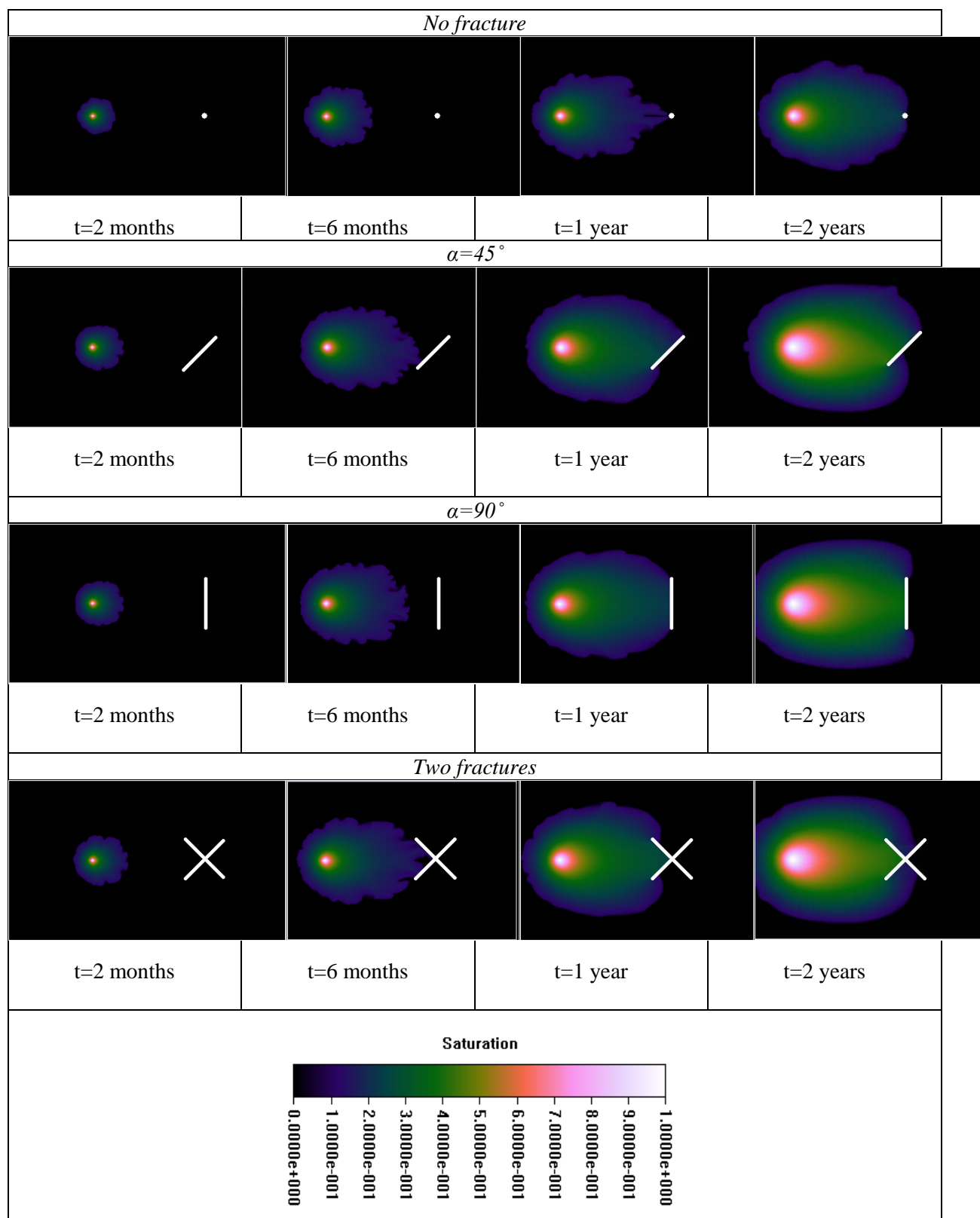

Fig. 12. The distribution of water saturation over time for the case of a single injection well in the calculated area

As can be seen from Figure 12, in the absence of a crack, the displacement front reaches the production well much later. The difference between the calculations with different angle of inclination of the crack is not significant. The case when two cracks do not have significant differences from the cases when there is one well.

a)
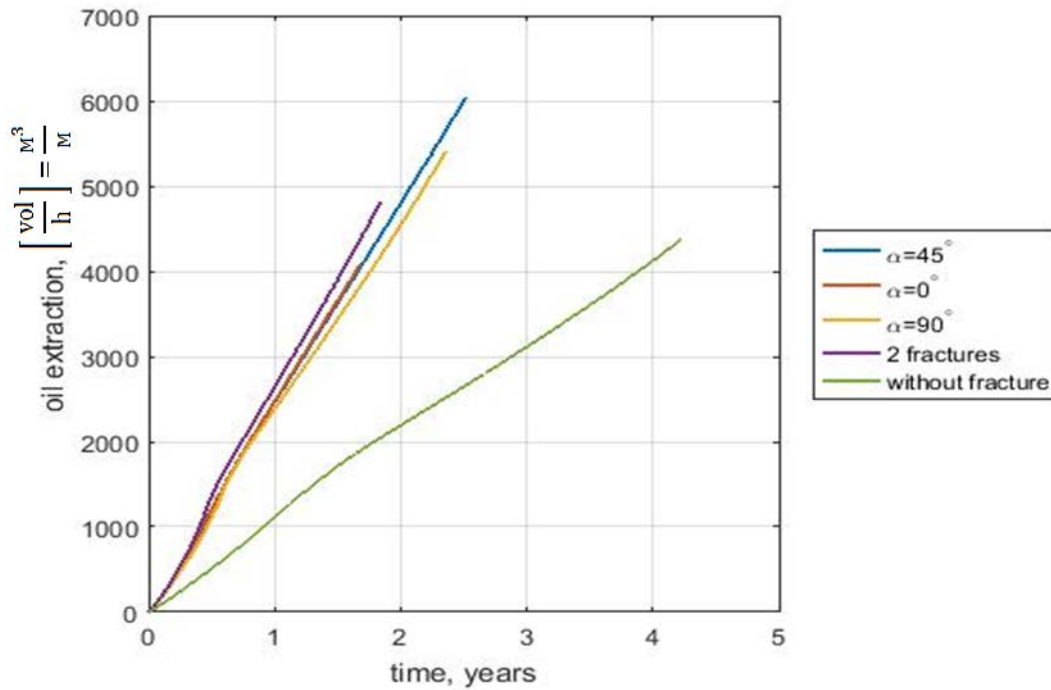
b)
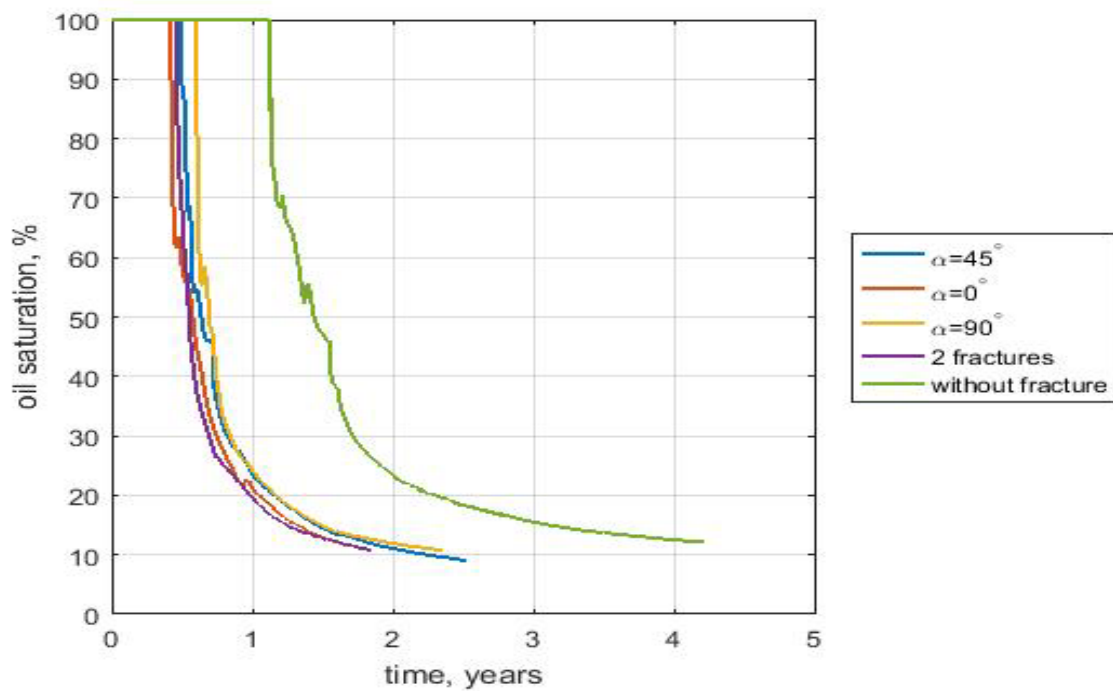
Fig. 13. a) Total oil production, in units of m^3 per meter of thickness; b) The share of the oil phase in production. The green curve corresponds to the case when the fracture is absent, blue is one fracture ($\alpha = 45°$), red is one fracture ($\alpha = 0°$), yellow is one fracture ($\alpha = 90°$), purple is two fractures

As can be seen from Figure 13, the fastest production occurs for two cracks. In the case when the fracture is one, its position is important - the case when the fracture is oriented perpendicular to the line connecting the injection and production wells, production occurs more slowly. In the case of the absence of a crack, extraction occurs much more slowly than in other cases (≈2 times). At the same time, the quality of the extracted oil is significantly higher when there is no crack: the time elapsed before the breakthrough of water to the producing well is about twice as large and the share of the oil phase in the production is much higher. The worst quality oil in the case of two cracks.

Figure 14 shows the dependence of the total oil production on the content of the oil phase in production.
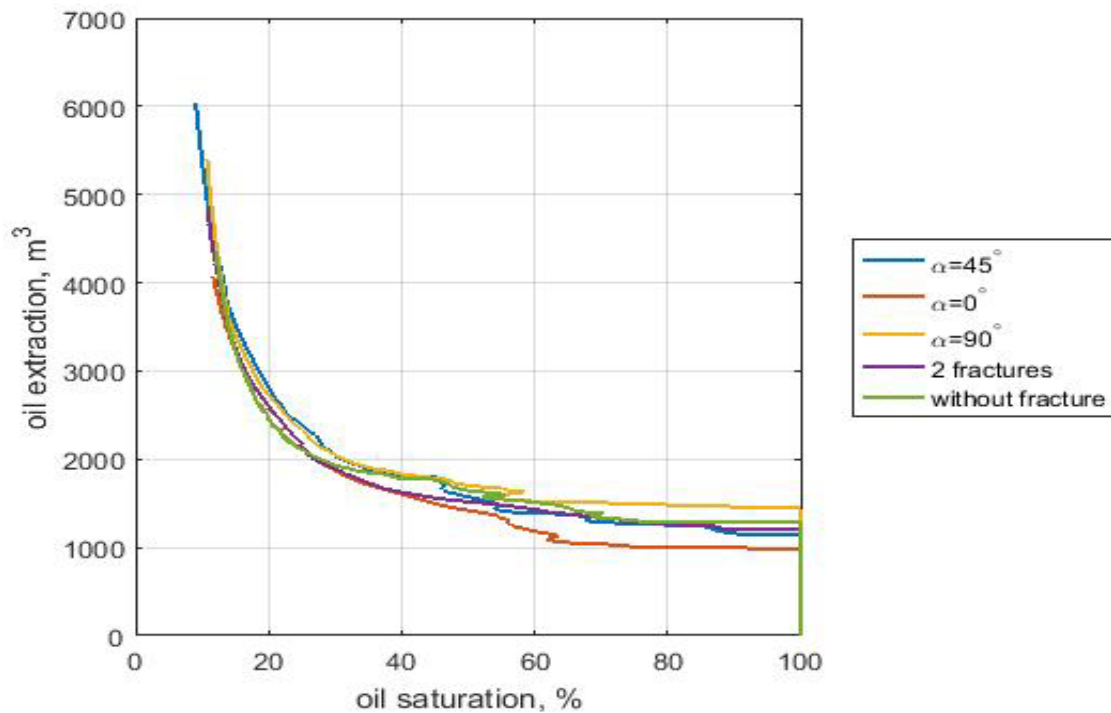

Fig. 14. The dependence of the total oil production on the share of the oil phase in production. The green curve corresponds to the case when the fracture is absent, blue is one fracture (α = 45°), red is one fracture (α = 0°), yellow is one fracture (α = 90°), purple is two fractures

According to Figure 14, at the initial stage of production, when the content of the oil phase is large, the position of the fracture affects the displacement process. In the case when α = 90°, the total oil production is significantly higher than when α = 0° with the same percentage of oil share in the production. Over time, when the share of the oil phase decreases, the curves in Fig. 14 approach each other and it can be considered that the number and position of the cracks does not affect the dependence of the total production on the share of the oil phase. If we assume that the well exploitation stops when the saturation of the oil phase in production drops to a certain value, then according to Fig. 14, the presence, number and position of fractures does not have a significant effect on the total oil production during the whole well exploitation period. At the same time, the presence of a crack and its "correct" location can speed up oil production by several times.

In the second series of calculations, an area of 300m × 300m is considered. In the corners of the area there are injection wells. In the center of the area there is a production

well. Near the production well there may be hydraulic fracturing. The parameters of the medium and the fractures, as well as the boundary conditions at the wells, coincide with the first series of calculations. Three calculations were carried out: 1 for the absence of a crack, 2 for different positions of two cracks. Figure 15 shows the water saturation at different points in time for each calculation (α is the angle of inclination of fractures).

Thus, the orientation of the fracture (α = 0° and α = 45°) does not affect the displacement process. In the case of the absence of a crack, the displacement front moves noticeably slower and does not reach the production well in the first year of its exploitation.
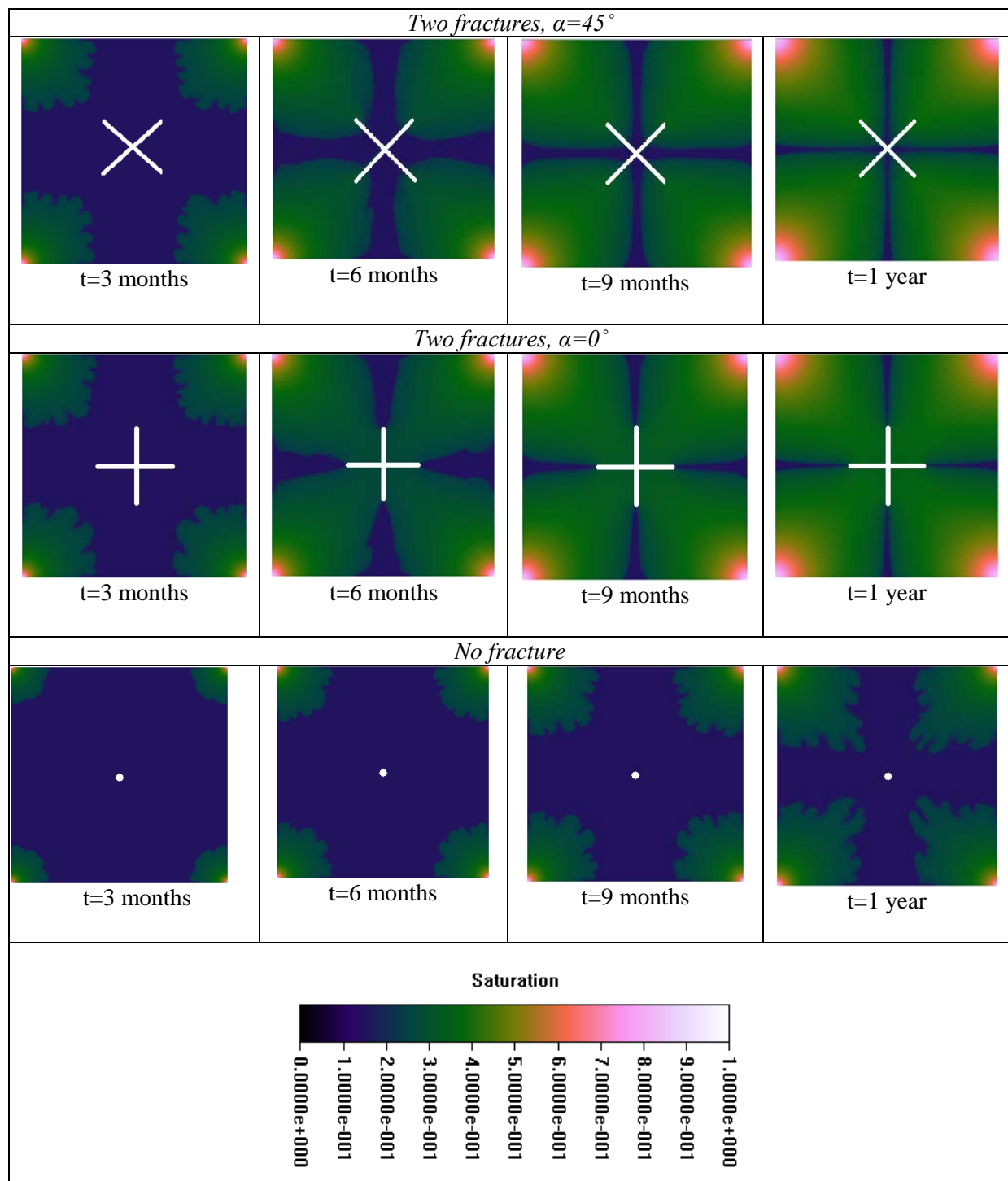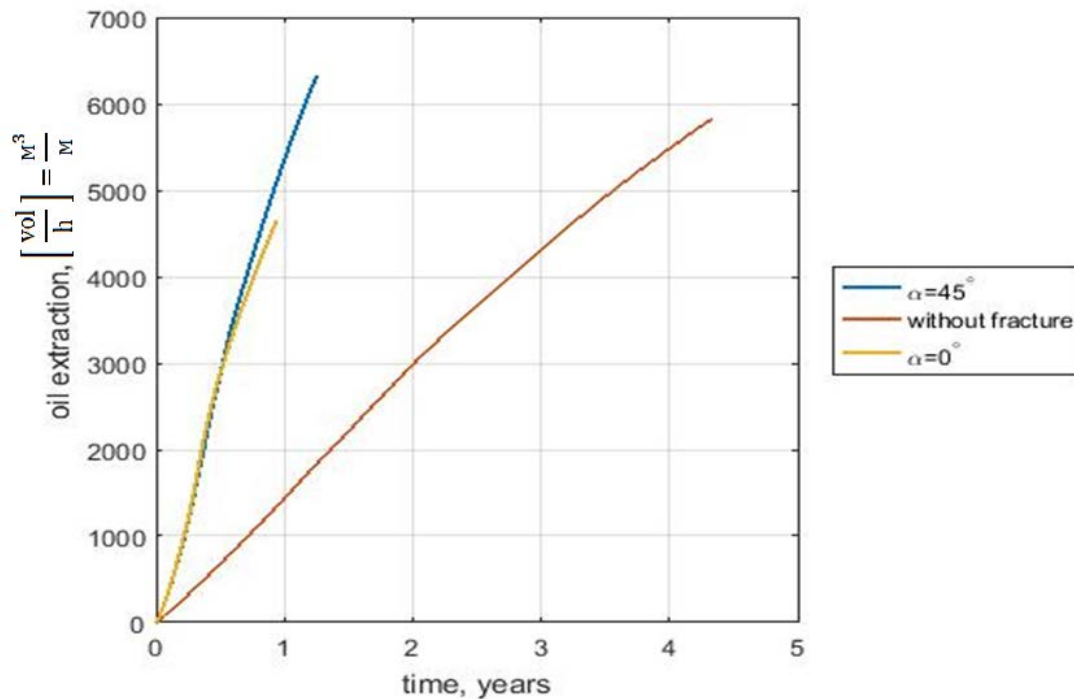

Fig. 15. The distribution of water saturation over time for the case of four injection wells in the calculated area
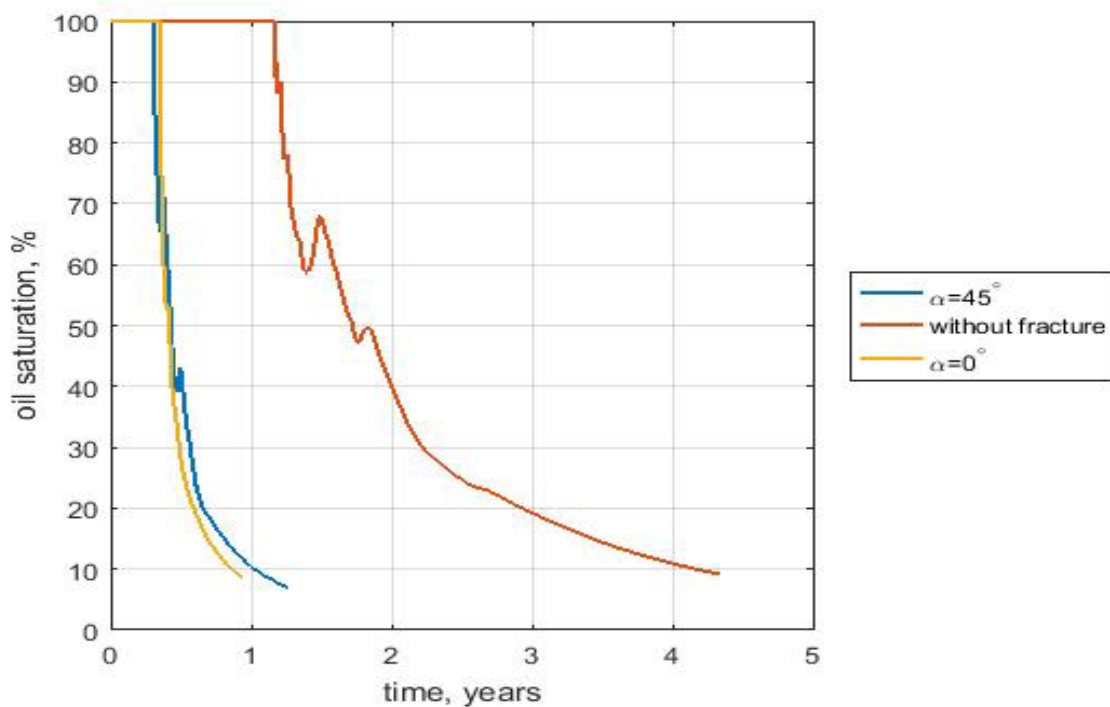
a)

b)

Fig. 16. a) Total oil production, in units of m^3 per meter of thickness; b) The share of the oil phase in production. The red curve corresponds to the case when there is no fracture, the blue one - two fractures ($\alpha = 45°$), the yellow one - two fractures ($\alpha = 0°$)

According to Figure 16, in the case when the fracture is absent, oil production is much slower. The orientation of fractures does not play a significant role. The quality of the extracted oil falls much faster if there are fractures.
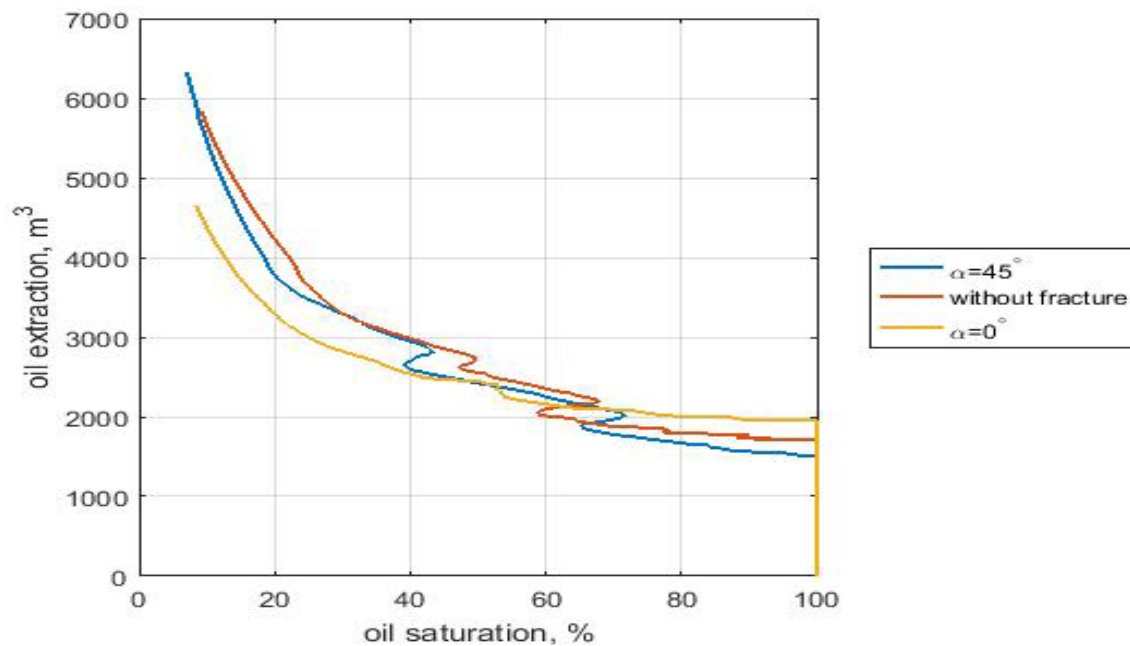
Fig. 17. The dependence of the total oil production on the share of the oil phase in production. The red curve corresponds to the case when there is no fracture, the blue one - two fractures ($\alpha = 45°$), the yellow one - two fractures ($\alpha = 0°$)

According to Figure 17, the orientation of the fractures affects the process of displacement. In the case when $\alpha = 0°$, with a small share of the oil phase in production, the total oil production is less than in other cases. The case when there are no fractures has no significant differences from the case when $\alpha = 45°$.

Thus, the study of the effect of hydraulic fracturing on the process of oil production showed that the presence of the fracture accelerates the displacement of oil, while the total amount of oil produced does not change. The orientation of a fracture can significantly affect the displacement dynamics. Thus, the fracture does not lead to an increase in oil recovery, but it intensifies it.

6. Capillary effects developed in microgravity investigation of seepage flows in porous media

The process of imbibition of viscous fluid into a porous medium depends essentially on capillary effects and instability, which may develop on the displacement front in case of multiphase flow. Accounting for capillary forces is critical for the description of the motion of liquids in porous media. The study of the capillary effects under ordinary conditions is difficult because of the significant effect of gravity on the seepage process. Therefore, was considers the flow of liquids in a porous medium under microgravity conditions during parabolic flights. The experimental data are compared with the results of a three-dimensional numerical simulation of the multiphase seepage process.

Experiments on imbibition of a wetting fluid (water) in an artificial porous medium composed of glass spheres were performed during aircraft parabolic flights. The experimental techniques is described in details by Istasse, 2001. Here we will concentrate our attention on the peculiarities of seepage flow in a media containing permeability inhomogenity. The zones of different permeabilities were arranged in the experimental cells (Fig. 19) using glass balls of different diameters. Porous samples were hermetically confined inside the experimental cell, whose overall dimensions are $74 \times 50 \times 315$ mm^3. Each cell has a separate fluid reservoir made of a deformable plastic bag. The reservoir fluid capacity is sufficient to fill in totally the

porous sample. The experimental cell was connected at its bottom side to a cylindrical connector. This connector was 70 mm long, and it serves as hydraulic junction between the porous sample and the reservoir, filled in with a water-dye mixture. The diameter of the channel zone has been chosen large enough, i.e. 37mm, to allow reasonable fluid feeding to the porous medium during microgravity periods. During the flight, the capillary-driven seepage was video recorded, using a high-quality video magnetoscope. The back-light system allows to visualize the phase interface separating water and air.

Fig. 18. The experimental cell for artificial porous medium

In this paper we consider three experiments. In all cases, we consider the imbibition of fluid into the porous media that has been prewetted throughout previous parabolas. Zones with different permeability were formed by spheres with diameters of 2 and 6 mm. The artificial porous medium within each zone was composed of glass balls of the same diameter. Thus the permeability of the porous medium consisting of spheres(d=6mm) was $K1 = 0.85 \cdot 10^{-8}$ m^2, while permeability in the low permeable zone(d=2mm) was $K2 = 0.20 \cdot 10^{-8}$ m^2.
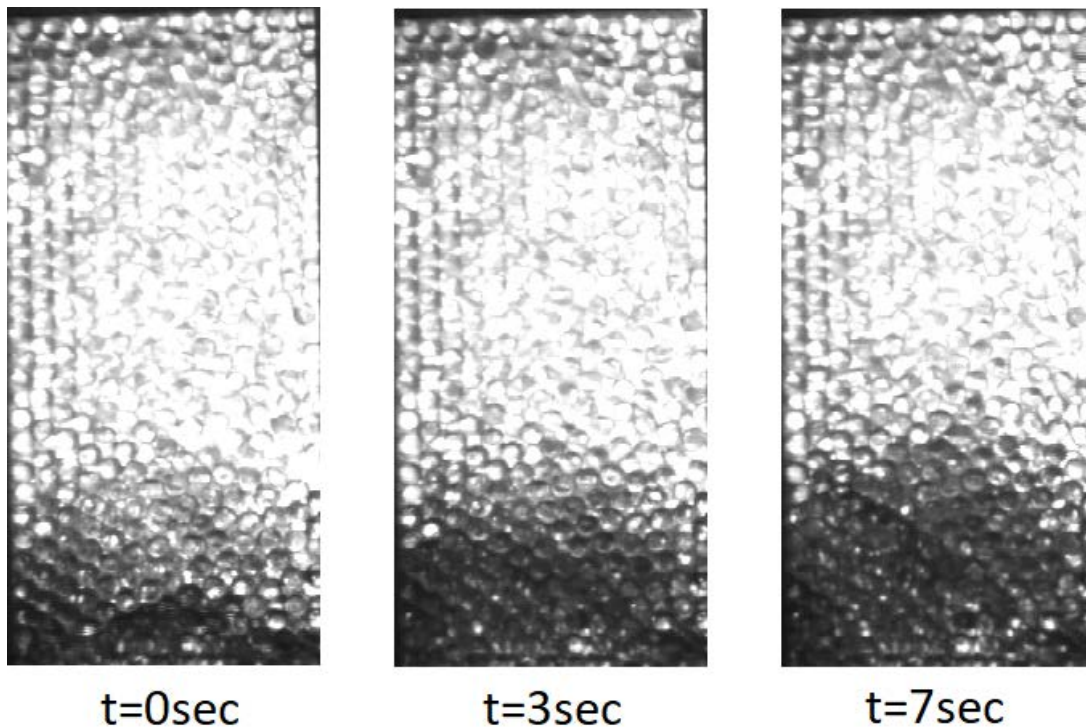

Fig. 19. The flow of liquid in a homogeneous porous medium under microgravity conditions

In the first experiment, the whole cell was filled with a homogeneous porous medium consisting of glass spheres with a diameter of 6 mm (Fig. 19). The graph (Fig. 22) shows the

position of the interface as a function of time. On reducing the gravity level the capillary driven imbibition of fluid into porous sample begins. During the observation period, the interface did not exceed the height of 40 mm.
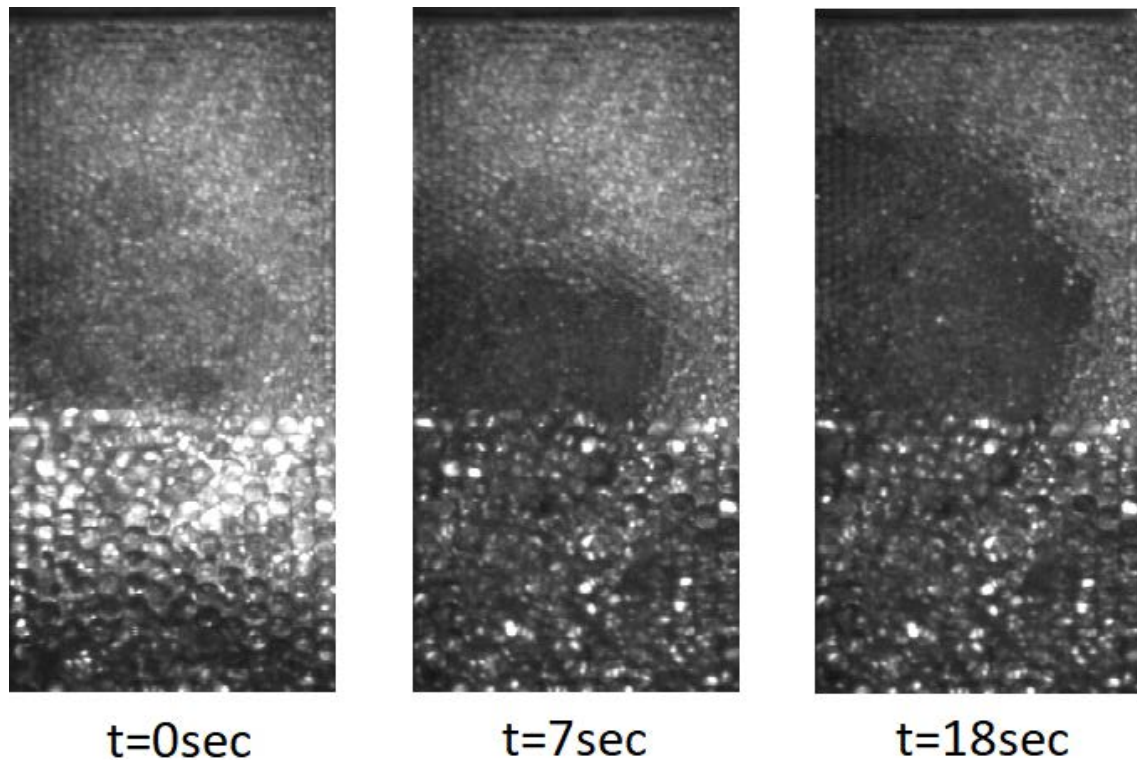

Fig. 20. The flow of liquid in an inhomogeneous porous medium under microgravity conditions

In the second experiment, the lower layer of the medium consisted of spheres with a diameter of 6 mm, the upper layer consisted of spheres of smaller diameter (2 mm) (Fig. 20). The position of the interface is shown in the graph (Fig. 23). The process of imbibition is analogous to the case of a homogeneous medium until a zone of low permeability is reached. When moving from a zone with high permeability to a zone with low permeability, the velocity of the interface movement increases substantially. After a while, the interface velocity again decreases. The acceleration of the imbibition front is explained by the fact that the capillary forces in the medium consisting of small spheres are higher.

In the third experiment there was a zone with a lower permeability in the cell filled in by spheres d = 6mm. The zone of lower permeability $30 \times 20 \times 30$ (mm^3) in the central part of the cell near the left wall was filled in with glass beads (d = 2 mm) (Fig. 21). The phase interface remains relatively flat in a homogeneous zone. On approaching the zone of lower permeability the interface becomes curved, the capillary creeping is faster in the zone of low permeability.
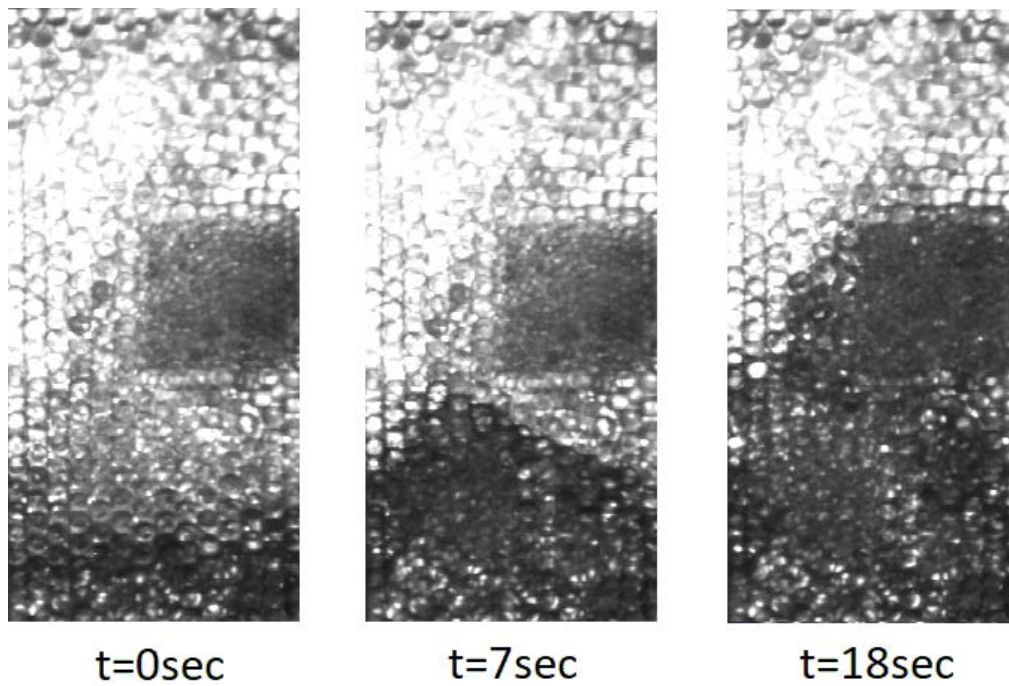
Fig. 21. The flow of liquid in a porous medium containing an insert with a low permeability under microgravity conditions
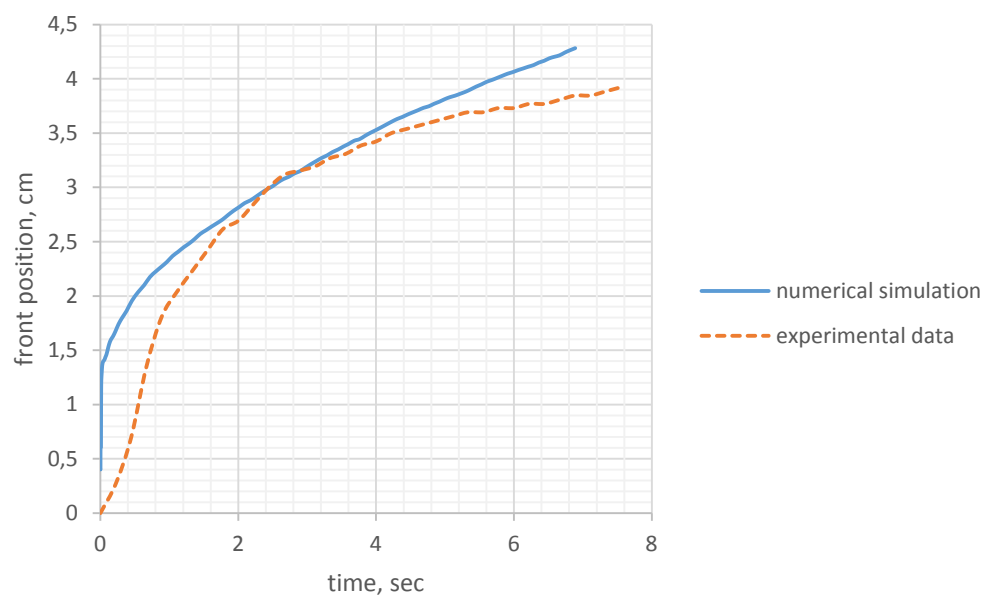

Fig. 22. The position of the interface as a function of time for a flow in a homogeneous medium
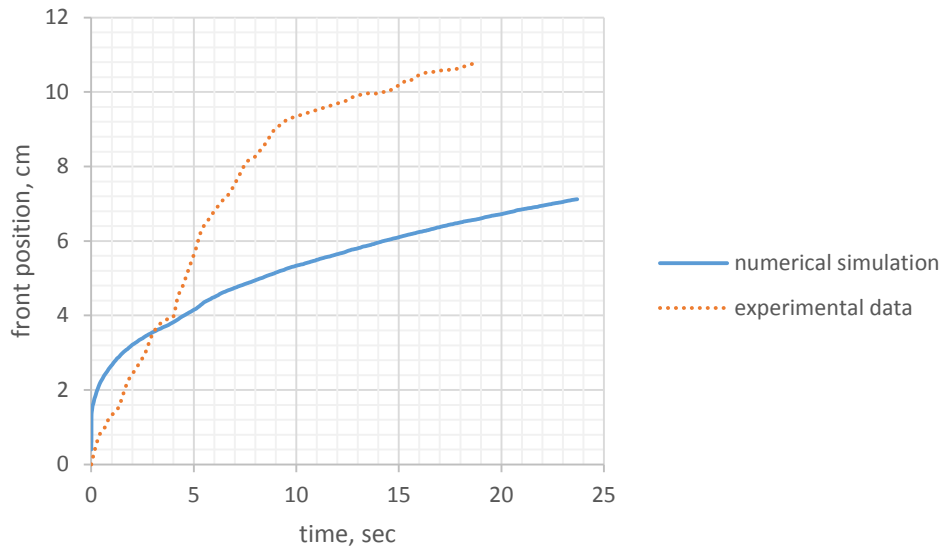
Fig. 23. The position of the interface as a function of time for a flow in an inhomogeneous medium

The flow of two incompressible fluids in porous media is considered, thermal effects are not taken into account. The imbibition is modeled by the Darcy law, taking into account the capillary effects at the boundary of the phases. Non-stationarity is taken into account. Permeability and porosity depend on the spatial co-ordinate and on the fluid pressure in the pores. The mathematical formulation of the problem describes the displacement by one fluid of another due to the pressure drop on the sides of the sample or due to a given flow on one side and also due to capillary effects.

The microgravity quality was very poor for the present experiments that does not permit us to perform quantitative comparison of results with the results of numerical modelling, which were carried out for ideal conditions. Nevertheless, the qualitative results of the calculation are similar to the experiment.

In the case of flow in a homogeneous medium (Fig. 22), the displacement is uniform gradually slowing down. In the experiment, the speed falls down more than in calculation. This is because the mathematical model does not take into account the acceleration of gravity g, which is close to zero in the experiment, but not equal to zero.

In the case of an inhomogeneous medium (Fig. 23), in the transition from a more permeable medium to a less permeable medium, acceleration of the imbibition front is observed. This corresponds to the results of the experiment.

The distribution of the saturation of the displacing liquid at different instants of time for the calculation, when the region contains an insert with a low permeability, is shown in Fig. 24. This calculation corresponds to the experiment shown in Fig. 21. In calculation, as in the experiment, having reached the insertion, the liquid begins to flow through the insert faster than in the zone with a higher permeability. The calculation also shows that the dispersion in a less permeable medium is higher.
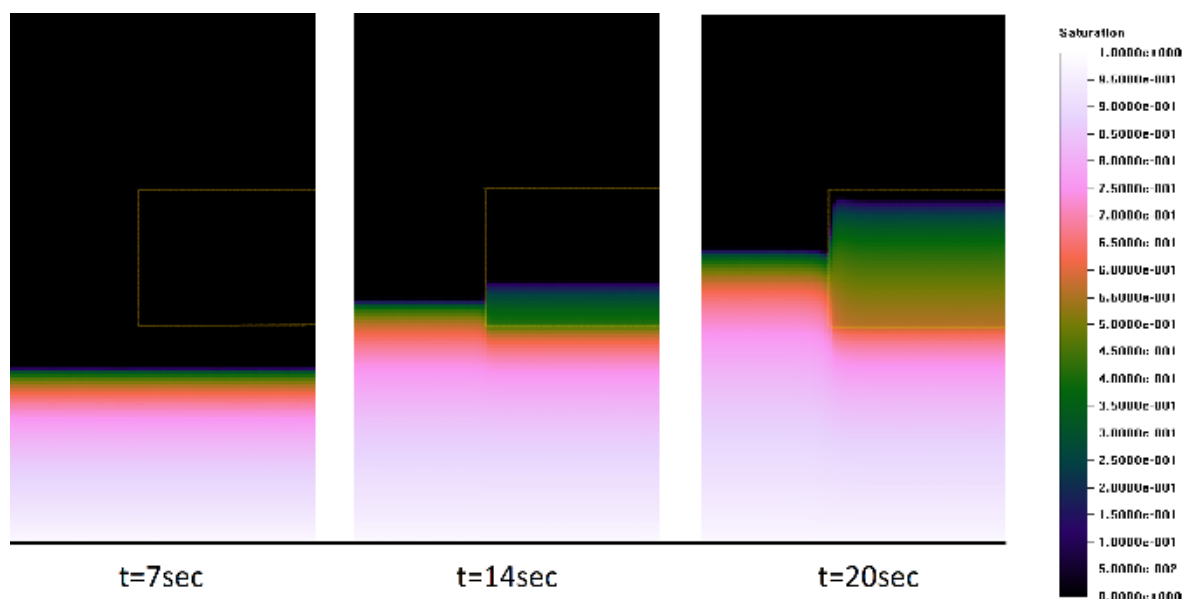
Fig. 24. The result of numerical modeling of fluid flow in the region containing an insert with a low permeability

In the future, it is planned to continue the development of mathematical and numerical models to create a high-performance supercomputing system necessary for predictive modeling of multiscale phenomena in underground hydrodynamics, where interdependent processes developed at different scales and their characteristic times differ by orders of magnitude [8,11,12].

7. Conclusions

Reliable evaluation of porosity and permeability based on tomography analysis needs regarding a large computational domain (better the whole specimen).

Evaluation of x-ray absorption coefficient threshold needs comparison of numerical simulation data with results of physical experiment with the same specimen.

Numerical simulation of core flow in a large computational domain needs distributed calculating systems.

Three dimensional numerical model for simulating unstable displacement flows of multi-phase fluids was developed. As a result of the comparison of data from supercomputer modeling of oil displacement from rock samples with a laboratory experiment to displace oil replacing liquids with water, it is possible to determine unknown parameters of the model, such as the capillary characteristics of the rock and saturating liquids.

Functional forms for simulating capillary forces can be developed in experiments on capillary driven imbibition into porous medium under microgravity conditions.

The total amount of recovered hydrocarbon does not depend on hydraulic fracturing, but the time of recovery is essentially shortened.

Hydraulic fracturing is a method for intensification of oil recovery, but not enhancing it.

The presence of entrapped fracturing fluid in a fracture and its vicinity lowers down the effectiveness of fracture.

Joint mechanic and economic studies are necessary to develop optimal design of hydraulic fracture minimizing its price and maximizing effectiveness.

References

[1] Smirnov NN, Tyurenkova VV, Kiselev AB, Nikitin VF. Filtration flows in a porous medium. *Northern region: science, education, culture.* 2015;2(32)(2): 74-86. (In Russian)

[2] Volpin SG, Smirnov NN, Kravchenko MN, Dieva NN. Modeling of pulse-wave processing of oil reservoirs by the method of thermogasochemical action. *Collection of scientific works of JSC "All-Russian oil and gas research Institute named after Akad. A.P. Krylov".* 2013;149: 127-137. (In Russian)

[3] Volpin SG, Saidgareev AR, Smirnov NN, Kravchenko MN, Korneev DA, Dieva NN. Prospects of application of wave technology thermogaschemical impact for EOR. *Oil industry.* 2014;1: 62-66.

[4] Volpin SG, Smirnov NN, Kravchenko MN, Dieva NN. Optimization of conditions for safe conducting of TGHV in oil fields. *Ecological Bulletin of Russia.* 2014;3: 17-21. (In Russian)

[5] Betelin VB, Smirnov NN, Stamov LI, Skryleva EI. Developing the structure of core pores based on processing of tomography data. *Proceedings in Cybernetics.* 2018;30(2): 87-92. (In Russian)

[6] Nikitin VF, Stamov LI. Three-Dimensional computational modeling of viscous fluid flow in the channel model of the core simulator. *Proceedings in Cybernetics.* 2016;4: 7-17. (In Russian)

[7] Nikitin VF, Stamov LI, Mikhalchenko EV. Three-Dimensional mathematical modeling of flow of viscous fluids in multiply connected system of channels and pores. *Proceedings in Cybernetics.* 2016;2: 127-137. (In Russian)

[8] Betelin VB, Nikitin VF, Smirnov NN, Mikhalchenko EV, Skryleva EI, Stamov LI, Tyurenkova VV. Computer core simulator – approaches and methods. *Proceedings in Cybernetics.* 2015;4: 33-44. (In Russian)

[9] Smirnov NN, Nikitin VF, Mikhailyuk MV, Timokhin PY, Tyurenkova VV, Stamov LI. Visualization of results of modeling of unstable displacement of oil from porous media. *Proceedings of SRISA RAS.* 2016;6(2): 34-37.(In Russian)

[10] Kozlov IV, Skryleva EI. Mathematical modeling and processing of the experiment on the displacement of oil by water from a Neocomian Sandstone. *Proceedings in Cybernetics.* 2016;2: 138-145. (In Russian)

[11] Dushin VR, Nikitin VF, Skryleva EI. Computational modeling of fluid displacement from porous media. *Proceedings in Cybernetics.* 2017;4: 62-82. (In Russian)

[12] Galkin VA, Gimranov RD, Spielmann VA. Russian Foundation for basic research in Yugra. The future of the region and Surgut - for high technology. *Proceedings in Cybernetics.* 2017;4: 11-16. (In Russian)